Cleaner Energy Systems 6 (2023) 100081

Contents lists available at ScienceDirect

Cleaner Energy Systems

journal homepage: www.elsevier.com/locate/cles

# Application of a flexibility estimation method for domestic heat pumps with reduced system information and data

Christian Baumann [a,b,*], Peter Kepplinger [a,b]

[a] illwerke vkw Endowed Professorship for Energy Efficiency, Research Center Energy, Vorarlberg University of Applied Sciences, Dornbirn, Austria
[b] Josef Ressel Centre for Intelligent Thermal Energy Systems, Vorarlberg University of Applied Sciences, Dornbirn, Austria

ARTICLE INFO

*Keywords:*
Flexibility estimation
Heat pump
Thermal energy storage
Intelligent thermal energy systems

ABSTRACT

Activation of heat pump flexibilities is a viable solution to support balancing the grid via Demand Side Management measures and fulfill the need for flexibility options. Aggregators as interface between prosumers, distribution system operators and balance responsible parties face the challenge due to data privacy and technical restrictions to transform prosumer information into aggregated available flexibility to enable trading thereof. Thereby, literature lacks a generic, applicable and widely accepted flexibility estimation method for heat pumps, which incorporates reduced sensor and system information, system- and demand-dependent behaviour. In this paper, we adapt and extend a method from literature, by incorporating domain knowledge to overcome reduced sensor and system information. We apply data of five real-world heat pump systems, distinguish operation modes, estimate power and energy flexibility of each single heat pump system, proof transferability of the method, and aggregate the flexibilities available to showcase a small HP pool as a proof of concept.

## 1. Introduction

The growing share of intermittent renewable energy generation in the electrical grid increases the need for flexibility options (Jensen et al., 2017). Therefore, aggregation and utilization of demand side flexibilities becomes increasingly important to help stabilizing the grid, and hence accelerate the integration of sustainable and clean energy production (Chen et al., 2018). These two actions have to come along to support and really impact balancing the grid via Demand Side Management (DSM) measures. The aggregation enables the determination of the possible potential of the bundled flexibilities of the single systems and allows an aggregator to trade the available flexibility with market participants, such as distribution system operators, balance responsible parties, and prosumers themselves (Olivella-Rosell et al., 2018; Gade et al., 2022). To trade and activate the aggregated flexibility, the time dependency and the economic value have to be considered by the aggregator (Iria et al., 2019).

However, for the flexibility utilization, it is key to activate the possible potential of each single system on controller level (Arteconi and Polonara, 2018). Typical demand side flexibilities considered in literature are heat pump (HP) systems for space heating (SH) (Arteconi et al., 2013) or domestic hot water (DHW) supply (Kepplinger et al., 2015), which exhibit flexibility via building mass and thermal energy storage (TES) (D'hulst et al., 2015; Hewitt, 2012). Hewitt (2012) stated that the role of HPs cannot be underestimated in an effort to integrate greater amounts of electricity, since the dynamics of even relatively simple buildings already allow a degree of thermal management and flexibility.

To utilize the HP flexibility on controller level, the community clearly fosters Model Predictive Control (MPC) approaches as solution (Kuboth et al., 2019, 2020; Pean et al., 2019; Baumann et al., 2023). Thereby, field tests have been executed to show the DSM potential for DHW and/or SH use. Kuboth et al. (2019, 2020) operated two identical test rig setups each consisting of a HP with 500 l TES for SH use to compare MPC to a hysteresis strategy in a short-term (5 days) and a long-term investigation (125 days). Both investigations achieved load shifting while reducing cost and increasing efficiency. Likewise, Pean et al. (2019) compared a MPC approach to a hysteresis strategy by deployment of test rig comprising an HP for SH and DHW including a 200 l TES for DHW use only. Within a three-day test period, results showed the load shifting potential with a cost reduction and a minor increase in electrical energy consumption. In a previous study

* Corresponding author at: illwerke vkw Endowed Professorship for Energy Efficiency, Research Center Energy, Vorarlberg University of Applied Sciences, Dornbirn, Austria.
*E-mail address:* christian.baumann@fhv.at (C. Baumann).

https://doi.org/10.1016/j.cles.2023.100081
Received 20 October 2022; Received in revised form 9 May 2023; Accepted 15 July 2023
Available online 4 August 2023

(Baumann et al., 2023), we operated a test rig consisting of a HP with 200 l TES for DHW use to also compare a MPC to a hysteresis strategy. Results of the one weekly test period showed 1) loads have been shifted to low price periods and 2) cost and energy reduction, as well as efficiency increase have been achieved. Even though literature shows that an utilization of the potential is possible under laboratory settings, the implementation in real-world systems in the field is still a challenge to overcome. Therefore, the flexibility itself has to be determined based on existing historical data. Hence, the challenge also lies in the estimation of the flexibility under these real-world settings.

On aggregation level, the aggregator uses the information from the prosumers, which are system- and demand-dependent. In literature, studies widely consider perfect knowledge of prosumer data to determine and aggregate demand side flexibility (Iria et al., 2019). In reality, all the prosumer information necessary are rarely available, which hinders flexibility estimation being the first step. Even more so, the access to prosumer data is difficult, as there are several obstacles to overcome: 1) data privacy, 2) lack of sensor and system information, and 3) cost for sensor retrofit and energy management systems (You et al., 2021; Zeiselmair and Köppl, 2021).

Further, a unique definition to quantify flexibility does not exist as opposed to the controller level (Chen et al., 2018; Clauß et al., 2017; Li et al., 2021). Li et al. (2021) show that literature provides more than 61 different flexibility definitions regarding aspects, such as comfort, emissions, cost, duration, power, and energy. Only 58% of the definitions have a sufficient mathematical formulation, where 85% of the quantification contains synthetic data and simulation, and less than 2% use real data. Furthermore, it is shown that the flexibility quantification is mostly considered in the building sector, where HPs cover about 26% of all energy resources, TES and thermal mass as a passive storage capacity represent over 50% of the associated facilities. An in-depth view on studies considering in particular HP flexibility estimation methods (Arteconi and Polonara, 2018; D'hulst et al., 2015; Fischer et al., 2017; Nuytten et al., 2013; Devriese et al., 2019; Marijanovic et al., 2022; Stinner, 2018) confirms that real-world settings and application with reduced sensor information are rarely included (Devriese et al., 2019). However, even the studies considering power and energy flexibility for HPs differ. Arteconi and Polonara (2018) illustrate that flexibility is mostly characterized by: amount of power change, duration of change, rate of change, response time, shifted load, and maximum hours of load shifted. Additionally, the authors assess the potential during operation time with the parameters temporal flexibility, power capacity, and energy shifted, while considering demand response control signals. Similar to Arteconi and Polonara (2018), Fischer et al. (2017) introduce the flexibility parameters maximum power, mean power, shiftable energy, duration time, and regeneration time for a heat pump pool. Further, the authors suggest duration of activation and regeneration as new flexibility parameters to get insights on shifting cycles. Nuytten et al. (2013) develop a more generic method to separate flexibility into a forced and delayed component. Results show that for HPs including a TES, the storage capacity has an almost linear influence on flexibility. Though, no distinction between SH and DHW was made.

The most promising definition and overview is provided in the PhD thesis of Stinner (2018). He develops a generic estimation method to distinguish between temporal, power and energy flexibility considering the cyclic behaviour of the TES. To estimate the flexibility, the method relies on perfect knowledge of a single prosumer system. However, the work neither distinguishes between DHW and SH use, nor considers the integration of reduced sensor and system information of real-world HP systems. As HP systems often comprise several modes of operation to provide heat for DHW and SH use, a viable approach needs to consider this. Reduced sensor information is often neglected in literature, assuming the rapid expansion of energy management systems dealing with this problem.

To summarize, literature lacks a transferable flexibility estimation method for HPs, which distinguishes DHW and SH use, deals with reduced sensor and system information, and considers system- and demand-dependent behaviour. Further, the study should estimate system characteristics and apply the method by incorporating real-world HP data and aggregate the estimated HP flexibilities.

We want to overcome this lack and contribute the following aspects to the community:

- Extension of a method from literature for flexibility estimation by considering reduced sensor and system information, as well as system- and demand-dependent behaviour.
- Application of the method developed to real-world HP data for a pool of different HP systems to prove the transferability.
- Analysis of seasonal influences on the HP flexibilities and of the dependence on thermal energy storage management.
- Aggregation of estimated HP flexibilities to provide a proof of concept.

We achieve this by adaptation and extension of the method proposed by Stinner (2018) through incorporation of system knowledge to overcome the reduced sensor and system information. The historical data, available to a heat pump manufacturer and operator, provide the base to estimate the system characteristics, temporal, power and energy flexibility of real-world HP systems on aggregation level. The data does not cover state information on the refrigerant to allow for a detailed model of the refrigeration cycle. Therefore, we use a simplified refrigeration cycle model based on a compressor map. Via modeling a perfectly stratified thermal storage, we can distinguish the energy demand for DHW and SH.

We investigate a single HP system to show the application of the methodology and to give insight into the flexibilities of one particular system. Further, we determine and compare the flexibilities of different systems to give an overview on how the flexibility changes with respect to the system. Lastly, we aggregate the flexibility of the systems investigated, to showcase a small HP pool.

## 2. Methodology

In this Section, we establish the methodology to estimate the temporal, power and energy flexibility and distinguish into forced and delayed case. In Section 2.1, we give information about the real-world HP system. In Section 2.2, we discuss the data preprocessing based on data provided by a heat pump manufacturer and operator. Section 2.3 establishes a method for system characteristics estimation necessary to adapt the flexibility estimation method by Stinner in Section 2.4. There, we define the forced and delayed temporal flexibility case considering the assumptions in accordance to the real-world HP system. In Section 2.5, the method is extended to the most important power and energy flexibility definitions incorporating the temporal flexibility.

### 2.1. HP system overview

All real-world systems investigated are brine/water HPs from the Weitrona line of the HP manufacturer Weider Wärmepumpen GmbH including a stratified TES for DHW and SH, cf. Fig. 1. Every system is deployed in the small Central European region of Vorarlberg, Austria.

Normally, to apply a methodology to a real-world HP system, the specifics of the system, including the hydraulic scheme and sensor positions have to be taken into account, and, are of high importance. However, in reality one is confronted with data privacy and cost reductive measures by manufacturers, which leads to a lack of system information. Due to these reductive measures by manufacturers, the system comes without comprehensive metering of pressure, temperature, power, and flow. Instead, our approach only uses a given compressor's map of characteristics and those sensors which are needed for operation. Measurements available with a resolution of one minute include evaporation temperature, flow temperature, DHW temperature

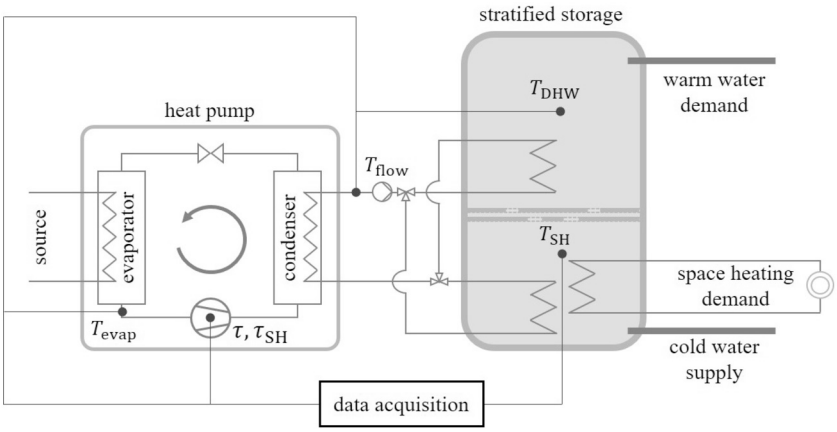


**Fig. 1.** Technical scheme of the HP system with all sensors and parameters available. Evaporation temperature $T_{evap}$ (°C) and operation times $\mathcal{T}$ (-) and $\mathcal{T}_{SH}$ (-) are measured inside the refrigeration cycle, whereas flow temperature $T_{flow}$ (°C), DHW temperature $T_{DHW}$ (°C) and SH temperature $T_{SH}$ (°C) are measured on the demand side.

**Table 1**
Overview of the HP systems investigated, including HP type, power consumption, and heating power at different supply temperatures, as well as the measured parameters.

| System | 1 | 2 | 3 | 4 | 5 |
|---|---|---|---|---|---|
| HP type (brine/water) | SW121 | SW71 | SW71 | SW71 | SW71 |
| Power consumption 35°C/55°C (kW) | 2.1 / 3.2 | 1.3 / 1.9 | 1.3 / 1.9 | 1.3 / 1.9 | 1.3 / 1.9 |
| Heating power 35°C/55°C (kW) | 10.5 / 9.6 | 5.9 / 5.4 | 5.9 / 5.4 | 5.9 / 5.4 | 5.9 / 5.4 |

(upper thermal capacitance), SH temperature (lower thermal capacitance), and operation times, cf. Fig. 1. These reduced information forces us to make assumptions on the calculation of electrical power $P_{el}$, cooling power $\dot{Q}_{cool}$, DHW demand $\dot{Q}_{DHW}$ and SH demand $\dot{Q}_{SH}$. On the one hand, electrical power and cooling power are determined by using the compressor's map of characteristics, on the other hand DHW and SH demand are also determined by using process knowledge and forward calculation.

### 2.2. Data preprocessing

We investigate five different HP systems with the specifications and parameters given in Table 1. Hereby, two types of compressors with different power ratings have to be considered. Further, data of six sensors are recorded, cf. Fig. 1. These sensors include the evaporation temperature $T_{evap}$ and the operation times $\mathcal{T}$, and $\mathcal{T}_{SH}$, which are measured at the heat exchanger outlet and on the compressor, respectively. On the demand side, the flow temperature $T_{flow}$, DHW temperature $T_{DHW}$ and SH temperature $T_{SH}$ are measured in the supply pipe of the TES, the upper thermal capacitance, and the lower thermal capacitance, respectively.

The data set of each of the five systems used, ranges in the time period from the 01/01/2021 to the 01/01/2022, and considers 3,153,600 data points each. Each data point refers to one minute. System latency leads to deviations of a few seconds in the date recorded. Further, system malfunctions can lead to the loss of single values. Therefore, we pre-process the data to:

- adapt the time stamps to a consistent one minute resolution,
- close small data gaps through a forward-fill,
- delete possible duplicated values,
- sort values according to the time stamp, and
- cast the data to the data type necessary.

Via a function developed, the compressor run time parameters are adjusted, such that later a distinction between DHW, SH and idle times can be made.

### 2.3. System characteristics estimation

In this chapter, we define the method to estimate the system characteristics necessary to further determine the flexibilities of the HP systems in Section 2.4 and 2.5. For each mode of operation, the electrical power $P_{el}$ and the cooling power $\dot{Q}_{cool}$ are determined via the compressor's map of characteristics. Further for each mode, the thermal capacity, the heat transfer characteristics, and the heat demand are estimated via process knowledge and forward calculation.

Defining operation times for DHW and SH via the measured compressor run times allows distinguishing between specific operation modes. The HP is either operated to supply heat for DHW or SH, or it is switched off, i.e., the total set of discrete-time steps $\mathcal{T} = \{t_1, \cdots, t_n\}$ can be divided into disjoint subsets,

$$\mathcal{T} = \mathcal{T}_{DHW} \sqcup \mathcal{T}_{SH} \sqcup \mathcal{T}_{OFF}. \quad (1)$$

To easily formulate relationships for both operation modes, we refer to the subscript $\cdot_M$, e.g., $\mathcal{T}_M$ can refer to $\mathcal{T}_{SH}$ or $\mathcal{T}_{DHW}$.

Polynomial regression of the compressor's map of characteristics is used to calculate the cooling power $\dot{Q}_{cool}$ and electrical power $P_{el}$ of the compressor, as no power or energy meter is available. Even though the compressor's map of characteristics is a well-established way in literature to determine the power of a HP, one has to consider that the power estimated can deviate from the real performance of the HP. However, since the European standard EN 14511-3:2022 allows a power deviation of 5% for an HP compressor and we further compare different HP systems with each other, these minor deviations from the compressor's map of characteristics to the real HP performance can be neglected (EN 14511-3:2022, 2022). Hence, the required power is estimated by using the operation times $\mathcal{T}_M$ and the polynomials are given by the manufacturer based on data recorded on a standardized test-rig for several operating points. The compressor's map of characteristics to estimate electric power, and cooling power is given as a third degree polynomial in condensation temperature $T_{cond}$ and evaporation temperature $T_{evap}$.

$$P_{\mathrm{el},M} = C_0 + C_1 T_{\mathrm{evap}} + C_2 T_{\mathrm{flow}} + C_3 T_{\mathrm{evap}}^2 + C_4 T_{\mathrm{evap}} T_{\mathrm{flow}} + C_5 T_{\mathrm{flow}}^2 + C_6 T_{\mathrm{evap}}^3 + C_7 T_{\mathrm{flow}} T_{\mathrm{evap}}^2 + C_8 T_{\mathrm{evap}} T_{\mathrm{flow}}^2 + C_9 T_{\mathrm{flow}}^3, \quad (2)$$

$$\dot{Q}_{\mathrm{cool},M} = C_0 + C_1 T_{\mathrm{evap}} + C_2 T_{\mathrm{flow}} + C_3 T_{\mathrm{evap}}^2 + C_4 T_{\mathrm{evap}} T_{\mathrm{flow}} + C_5 T_{\mathrm{flow}}^2 + C_6 T_{\mathrm{evap}}^3 + C_7 T_{\mathrm{flow}} T_{\mathrm{evap}}^2 + C_8 T_{\mathrm{evap}} T_{\mathrm{flow}}^2 + C_9 T_{\mathrm{flow}}^3. \quad (3)$$

Since the condensation temperature is not recorded by measurement, the flow temperature is used as an estimate of the condensation temperature, i.e. $T_{\mathrm{cond}} \approx T_{\mathrm{flow}}$.

Then, at each time step $t$, the heating power $\dot{Q}_{\mathrm{in}}$ for both modes of operation, DHW and SH, is calculated as follows,

$$\dot{Q}_{\mathrm{in},M}(t) = P_{\mathrm{el},M}(t) + \dot{Q}_{\mathrm{cool},M}(t). \quad (4)$$

Determination of heat transfer characteristics $(UA)_{\mathrm{DHW}}$ and $(UA)_{\mathrm{SH}}$ of the TES, as well as the thermal storage capacities $C_{\mathrm{DHW}}$ and $C_{\mathrm{SH}}$ is based on the assumption of a perfectly stratified storage (stratification switches) leading to the following energy balances for each operation mode,

$$\frac{C_M dT_M}{dt} = \dot{Q}_{\mathrm{in},M}(t) - \dot{Q}_{\mathrm{loss},M}(t) - \dot{Q}_{\mathrm{dem},M}(t). \quad (5)$$

We assume the heat flow from the HP to the storage to take place in the respective storage layer.

TES capacities $C_{\mathrm{DHW}}$ and $C_{\mathrm{SH}}$ are determined by identifying the shortest heating period for which no demand occurs, assuming losses to be negligible,

$$C_M = \frac{\sum_{t_1}^{t_2} \dot{Q}_{\mathrm{in},M}(t)\Delta t}{(T_M(t_2) - T_M(t_1))(t_2 - t_1)}, \quad (6)$$

where $(t_1, t_2) = \arg \min_{t_1,t_2 \in \mathcal{T}_M} t_2 - t_1$, (7)

s. t. $T_M(t_2) = T_{\mathrm{up},M}$, (8)

$T_M(t_1) = T_{\mathrm{low},M}$, (9)

$\dot{Q}_{\mathrm{in},M}(t) > 0 \ \forall t \in [t_1, t_2]$. (10)

Here, $T_{\mathrm{up},M}$ and $T_{\mathrm{low},M}$ refer to the upper and lower set point temperature, respectively.

Analogously, in Eq. (11), heat transfer characteristics $(UA)_{\mathrm{DHW}}$ and $(UA)_{\mathrm{SH}}$ have been determined, by using maximum duration non-heating periods, assuming to reflect no demand,

$$(UA)_M = \frac{C_M(T_M(t_2) - T_M(t_1))}{(T_M(t_2) - T_\infty)(t_2 - t_1)}, \quad (11)$$

where $(t_1, t_2) = \arg \max_{t_1,t_2 \in \mathcal{T}_{\mathrm{OFF}}} t_2 - t_1$, (12)

s. t. $T_M(t_1) = T_{\mathrm{up},M}$, (13)

$T_M(t_2) = T_{\mathrm{low},M}$, (14)

$\dot{Q}_{\mathrm{in},M}(t) = 0 \ \forall t \in [t_1, t_2]$. (15)

Reformulating Eq. (5) with parameters $(UA)_M$ and $C_M$ allows determining the demand as follows,

$$\dot{Q}_{\mathrm{dem},M}(t) = \dot{Q}_{\mathrm{in},M}(t) - (UA)_M\left(T_M(t) - T_\infty(t)\right) - C_M\left(T_M(t + \Delta t) - T_M(t)\right), \forall t \in \mathcal{T}_M. \quad (16)$$

The maximum available TES capacity is determined by

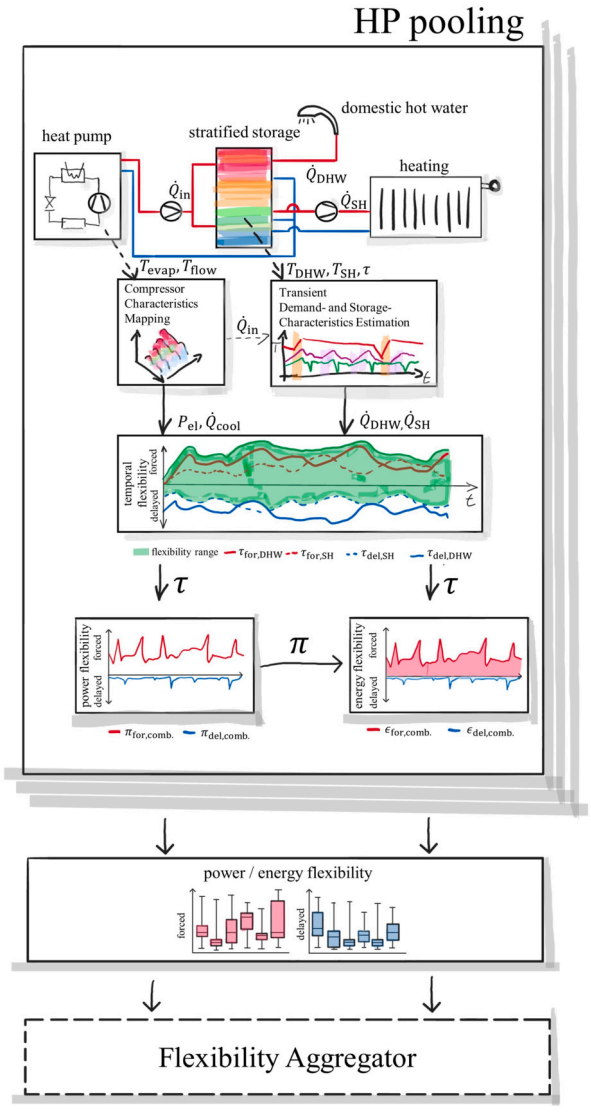


**Fig. 2.** Graphical abstract of the method proposed to derive a temporal, power and energy flexibility and to aggregate flexibilities for a flexibility aggregator.

$$E_{\max,M} = C_M \Delta T_M = C_M(T_{\mathrm{up},M} - T_{\mathrm{low},M}). \quad (17)$$

To estimate the maximum heating power and energy for the present mode of operation, the highest value in data is chosen,

$$\dot{Q}_{\max,M} = \max_{t \in \mathcal{T}_M} \dot{Q}_{\mathrm{in},M}(t), \quad (18)$$

$$Q_{\max,M} = \max_{t \in \mathcal{T}_M} \dot{Q}_{\mathrm{in},M}(t)\Delta t. \quad (19)$$

Determination of the specific parameters results in a one hour resolution of the later results.

### 2.4. Temporal flexibility

According to Stinner (2018), temporal flexibility can be divided into forced and delayed temporal flexibility. The former refers to the maximum operation time of the HP until the storage is fully charged, the latter to the time until full depletion of the storage. We adapt this method by distinguishing into DHW and SH use for the two thermal capacities, to derive a combined forced and delayed flexibility range for the overall HP system, see Fig. 2. Within the flexibility range the user comfort (for DHW or SH use) is ensured at all times, as the HP

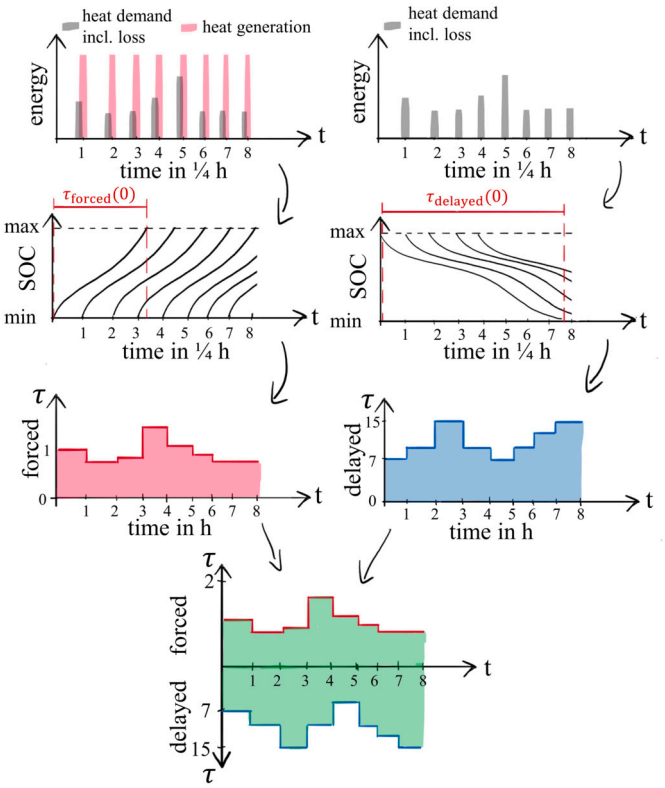


**Fig. 3.** Schematic of the estimation methodology for forced (left) and delayed (right) temporal flexibility, according to Stinner (2018).

power, the HP operation, and the demands are considered. This distinction allows a detailed view on the system compared to methods from literature. The proposed method not only allows to be transferred to other HP systems but also provides the basis for a cloud-based system to estimate the flexibility of a fleet of HPs. In the following sections, the necessary steps are explained in detail.

Stinner (2018) defines the forced temporal flexibility for each time step as the period necessary to fully charge the TES by the surplus power of the HP working at maximum power, cf. Fig. 3. Hence, repeating this process for every time step $t$ with an assumed discharged TES at the beginning, the forced temporal flexibility $\tau_{for,M}(t_0)$ can be determined by solving

$$\sum_{t=t_0}^{\tau_{for,M}(t_0)} Q_{max,M} - Q_{dem,M}(t) - Q_{loss,M}(t) \overset{!}{\geq} E_{max,M}. \tag{20}$$

In the same way, the delayed temporal flexibility is defined as the period the HP can be switched off until the full energetic depletion of the TES is reached from a fully charged state. Heat demand and heat losses lead to the depletion of the TES (Fig. 3, right). Repeating this process for every time step $t$, the delayed temporal flexibility $\tau_{del,M}(t_0)$ can be determined by solving

$$\sum_{t=t_0}^{\tau_{del,M}(t_0)} Q_{dem,M}(t) + Q_{loss,M}(t) \overset{!}{\geq} E_{max,M}. \tag{21}$$

A feasible operation has to take into account both constraining demands, resulting in the combined flexibility range, cf. Fig. 2. Since generated heat input is operation mode dependent, both thermal capacities are exploited. Hence, both forced flexibilities accumulate to a combined function describing the upper bound of the flexibility range. Opposing, delayed temporal flexibility as lower bound of the flexibility range takes the minimum available time of both DHW and SH into account. Assuming the decision for full energetic depletion of the chosen storage capacity, only one limit can be exploited at a time, otherwise comfort and system boundaries being violated. These operation constraints apply further for power and energy flexibility to estimate the overall system's flexibility.

### 2.5. Power and energy flexibility

The temporal flexibility estimation provides the basis for further calculation of power and energy flexibility. The derived combined temporal flexibility range from Section 2.4 provides the input in this Section for the calculation of the power and energy flexibility. The combined temporal flexibility range is taken to consider the overall HP system's flexibility and the different operation modes. Hence, all parameter inputs are considered for the combined case. The power curves are determined by comparing maximum electrical power $P_{max}$ (forced) and minimum electrical power $P_{min}$ (delayed) to the reference case $P_{ref}$, which represents the measured power by the HP. The resulting power curve equals to the flexible power available. Similarly to Eq. (18), the maximal electrical power can be calculated as follows,

$$P_{max} = \max_{t \in \mathcal{T}} P_{el}(t). \tag{22}$$

Both power flexibilities can be described as follows, starting at time $t$,

$$\pi_{flex,for}(t, \xi - t) = P_{max}(\xi) - P_{ref}(\xi)$$
$$\text{where } t \leq \xi \leq t + \tau_{for}(t), \tag{23}$$

$$\pi_{flex,del}(t, \xi - t) = P_{ref}(\xi) - P_{min}(\xi)$$
$$\text{where } t \leq \xi \leq t + \tau_{del}(t). \tag{24}$$

As in most cases the minimum electrical power will be zero, the delayed flexibility power curve equals to the reference curve. While the facilitation of the power (forced or delayed) is also dependent on the opposite process (whether discharging or charging), the whole storage cycle is taken into account. To incorporate the storage cycle, the cycle power flexibilities can be described by,

$$\pi_{cycle,for}(t) = \begin{cases} \frac{\int_0^{\tau_{for}(t)} \pi_{flex,for}(t,\xi)\,d\xi}{\tau_{for}(t)+\tau_{del}(t)+\tau_{for}(t))} & , \text{if } \tau_{for}(t) > 0 \\ 0 & , \text{if } \tau_{for}(t) = 0 \end{cases}, \tag{25}$$

$$\pi_{cycle,del}(t) = \begin{cases} \frac{\int_0^{\tau_{del}(t)} \pi_{flex,del}(t,\xi)\,d\xi}{\tau_{del}(t)+\tau_{for}(t)+\tau_{del}(t))} & , \text{if } \tau_{del}(t) > 0 \\ 0 & , \text{if } \tau_{del}(t) = 0 \end{cases}. \tag{26}$$

Energy flexibility is used, to compare different flexibility options to each other, being a combination of temporal flexibility and power flexibility. As the usage of flexibility in preceding periods affects the availability of the flexibility in the current state, it is necessary to take the storage cycles in account to derive quantities reflecting these dependencies. The resulting energy flexibility value indicates the maximum possible energy that can be delivered in forced or delayed operation over the year,

$$\epsilon_{for,year} = \int_0^{t_{year}} \pi_{cycle,for}(\xi)\,d\xi, \tag{27}$$

$$\epsilon_{del,year} = \int_0^{t_{year}} \pi_{cycle,del}(\xi)\,d\xi. \tag{28}$$

The methodology presented extended the method by Stinner (2018) by distinguishing the thermal storage capacities and operation modes into DHW and SH use and, thereby, deriving a combined temporal flexibility range. With the combined temporal flexibility range, we are able to estimate the available power- and energy flexibility of the overall single HP system considering the different operation modes. The estimation of the heat transfer characteristics and the thermal capacities of each mode is enabled through integration of process knowledge and forward calculation. Of particular interest are the power- and energy

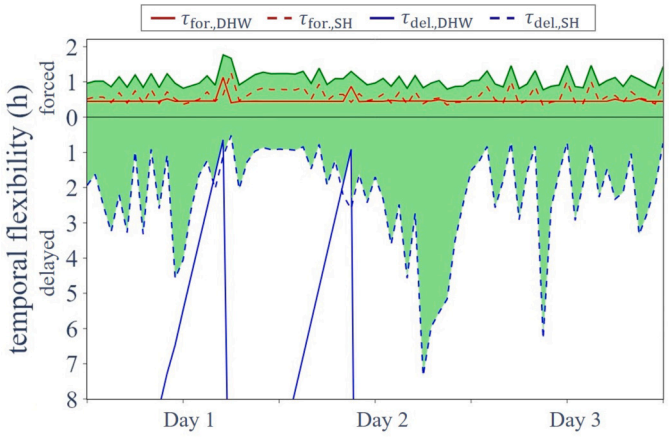


**Fig. 4.** Determined forced and delayed temporal flexibility for DHW-, SH- and the combined mode. Forced temporal flexibility (red) and delayed temporal flexibility (blue) shown for DHW/SH mode (solid/dashed). Combined temporal flexibility range (green area) derived by boundary conditions of forced and delayed temporal flexibility of DHW and SH.

flexibility, as the former is a measure on how much imbalance could be compensated, and the latter a measure on how long the power flexibility would be available. The methodology presented enables flexibility aggregators to not only estimate the available power- and energy flexibility of single HP systems, but also aggregate the flexibilities of a fleet of HP systems. In this study, the aggregation is enabled by accumulation of the flexibilities considered. The coincidence of HP systems operation in a fleet or quarter are not investigated in this study. As coincidence is caused by outside temperatures for SH and human behaviour for DHW, territorial near systems might tend to operate in similar time periods. On the one hand, this might offer even higher potential flexibility for the aggregator and, on the other hand, the possibility to shift loads for DSM.

## 3. Results and discussion

In Section 3.1, we investigate a single HP system to show the application of the methodology and to give insight into the flexibilities of one particular system. In Section 3.2, we determine and compare the flexibilities of different systems to give an overview on how the flexibility changes with respect to the system. Lastly, in Section 3.3, we aggregate the flexibility of all investigated systems to show how much aggregated flexibility a small HP pool can possibly provide.

Please note that the evaluated box plots of flexibility distributions with whiskers from minimum to maximum declare no outliers.

### 3.1. Single heat pump system

For the single system, we investigate a Weider Weitrona SW71 HP system.

Assuming a perfect stratification (stratification switches) leads to the determination of the thermal capacity $E_{\max,M}$ to be 3.75 kWh for DHW and 3.95 kWh for SH, respectively. Analogously, the heat transfer characteristic $(UA)_M$ is determined as 0.23 W/K for DHW and 1.11 W/K for SH, respectively.

Based on these values, iterative calculation of heat demand and heat loss for DHW and SH is implemented and leads to the necessary profiles. The flexibility estimation is based on a data set of one year.

In Fig. 4 the forced and delayed temporal flexibility, determined for DHW and SH are depicted for three consecutive days in winter. Combined forced temporal flexibility is derived by an accumulation of forced temporal flexibility for DHW and SH, shown as green curve. Thus, a maximum combined forced temporal flexibility of 1.8 hours can be determined. The possible forced temporal flexibility range lays within 0.8 and 1.8 hours. Analogously, finding the minimum available delayed temporal flexibility of DHW and SH leads to the opposing maximum available delayed temporal flexibility of the combined system. In the time series of the three consecutive days, a maximum delayed temporal flexibility of 7 hours can be determined. The possible delayed temporal flexibility range lays within 0.5 and 7 hours. Derived from these two ranges, the overall range lays within 1.8 hours forced and 7 hours of delayed temporal flexibility.

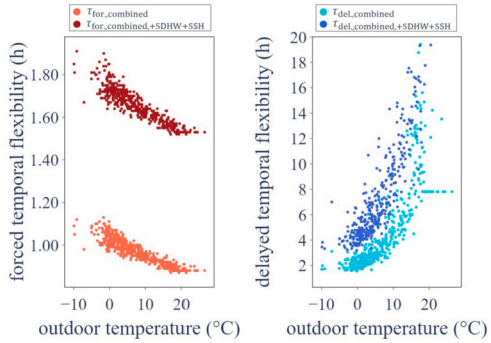


**Fig. 5.** Left: The daily mean of combined forced temporal flexibility plotted against the daily mean of outdoor temperature over a one year period. Right: The daily mean of delayed temporal flexibility plotted against the daily mean of outdoor temperature over a one year period.

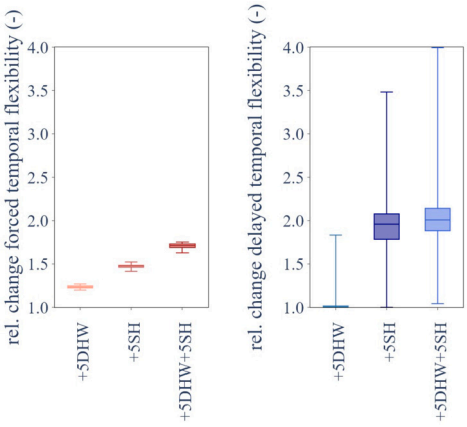


**Fig. 6.** Relative change of forced (left) and delayed (right) combined temporal flexibility considering different temperature spread scenarios of the thermal energy storage.

Considering possible forced and delayed temporal flexibility in more detail, four different scenarios for DHW and SH temperature spreads (+5K) are investigated: reference case, +5DHW, +5SH and +5DHW+5SH.

Fig. 5 (left) refers to the forced temporal flexibility, showing two of the scenarios investigated. The daily mean of forced temporal flexibility is plotted against the daily mean of outdoor temperature over a one year period. A decrease in the available forced temporal flexibility with rising outdoor temperatures for all scenarios considered is shown. The following average proportionality can be observed: 1.3 for +5DHW, 1.5 for +5SH and 1.8 for +5DHW+5SH, cf. Fig. 6 (left). Hence, the increase of the combined temperature spread +5DHW+5SH leads to the highest potential, followed by the +5SH, and the +5DHW scenario. Comparison of the +5DHW and the +5SH scenario shows a higher flexibility per Kelvin in the SH scenario, which can be accounted to the higher thermal capacity.

In contrast to forced temporal flexibility, an increase in the available delayed temporal flexibility with rising outdoor temperatures can be observed, cf. Fig. 5 (right). For delayed temporal flexibility, low SH use is related to higher outdoor temperatures and provides more available ca-

**Table 2**
Overview of the identified heat transfer characteristics and maximum thermal capacities of each HP system.

| System | 1 | 2 | 3 | 4 | 5 |
|---|---|---|---|---|---|
| $(UA)_{DHW}/(UA)_{SH}$ (W/K) | 0.35 / 0.63 | 0.23 / 1.11 | 0.26 / 1.48 | 0.23 / 0.48 | 0.26 / 0.85 |
| $E_{DHW}/E_{SH}$ (kWh) | 6.40 / 2.27 | 3.75 / 3.95 | 2.45 / 4.53 | 3.27 / 0.87 | 3.82 / 4.57 |

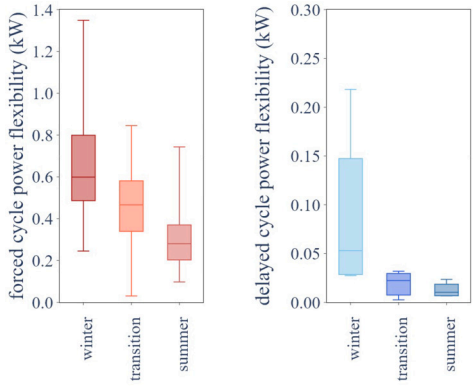


**Fig. 7.** Forced (left) and delayed (right) cycle power flexibility for winter, transition and summer season considering the cyclic behaviour of the thermal energy storage.

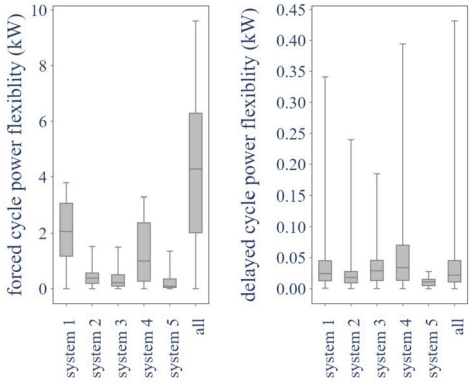


**Fig. 8.** Forced (left) and delayed (right) cycle power flexibility of the 5 systems considered, and aggregation of all systems for a one year period. The resolution of the cycle power flexibility considers the cyclic behaviour of the thermal energy storage.

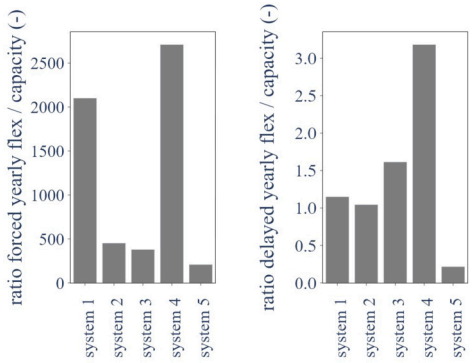


**Fig. 9.** Ratio of forced (left) and delayed (right) yearly energy flexibility to the available thermal capacity of all 5 systems. The ratio is displaying the amount of theoretically achievable loading and depletion cycles per year.

pacity. The highest flexibility of the scenarios investigated is observed in the combined +5DHW+5SH scenario. The following average proportionality can be observed: 1.1 for +5DHW, 2.0 for +5SH and 2.1 for +5DHW+5SH, cf. Fig. 6 (right).

Based on the temporal flexibility, the power flexibilities are calculated. Hence, forced and delayed cycle power flexibility are determined for a one year period and three consecutive days in winter, transition and summer season are compared, cf. Fig. 7. While a clear decay in average power flexibility is observed in both, forced and delayed case, the forced case shows high spreads from minimum to maximum in all seasons (left). Compared to the average values of each season (winter 0.6 kW, transition 0.5 kW and summer 0.3 kW), maximum values are doubling and minimum values are halving, respectively. In the delayed case the average power flexibility is about ten-fold smaller than in the forced case (winter 0.05 kW, transition 0.03 kW and summer 0.015 kW). Hence, the winter season shows in both cases the highest potential compared to the other two seasons. This can be attributed to the higher demand, as winter also includes SH use. The big difference in forced and delayed potential is the result of TES sizing, demand- and power injection times.

### 3.2. Comparison of multiple systems

We applied the method to five HP systems and investigated the power and energy flexibility available. The investigation is done to prove transferability, and to give an overview how the flexibility changes with respect to the system given. The flexibility estimation was done for a one year period. The HP specs with the parameters determined for the heat transfer characteristics and the maximum thermal storage capacity are shown in Table 2.

Fig. 8 shows box plots of forced and delayed cycle power flexibility. In the forced case (left), the power flexibility averages in system 2, 3, and 5 roughly around 0.2 kW, where maxima around 1.4 kW are recorded. However, system 1 and 4 deviate from all other systems with higher average values (2 kW and 1 kW) and maxima around 3.8 kW. Due to the lower thermal capacity for SH, most of the flexibility in these two systems comes from the thermal capacity for DHW, where the HP operates at higher temperatures and higher power. In the delayed case (right), box plots of all systems show average values around 0.02 kW. All other systems, apart from system 5, show maximum values of 10 to 20-fold the average. This high deviation can be contributed to high demands, as they cause high peaks in delayed cycle power flexibility.

To obtain a view on the utilization of the TES, the yearly available forced and delayed energy flexibility are calculated and compared to the TES capacity, cf. Fig. 9. Thereby, the ratio is an indicator on how often during one year the TES can be energetically fully loaded or depleted.

In the forced case, values of system 2,3 and 5 range between 210 and 450, whereas system 1 and 4 peak with values from 2100 to 2700 (left). This means for systems 2, 3, and 5, roughly only once per day the TES can be fully loaded with the surplus of HP power. In the delayed case, values of all systems range between 1.0 and 3.2, while system 5 shows the smallest value of 0.2 (right). For system 2, 3, and 5, one can observe that the involved components are not sized optimally with respect to each other and/or demand. Oversizing of the system components (TES, HP) with respect to demand, leads to higher flexibility. Results (Fig. 8 and 9) show that even though system specifications are similar, e.g., compressor class, available flexibilities differ because of the high dependency on the system setup and user behaviour, cf. system 2, 3, 4, and 5. The higher amount of loading cycles in system 1 and 4 is, among others, a result of the lower thermal capacity for SH.

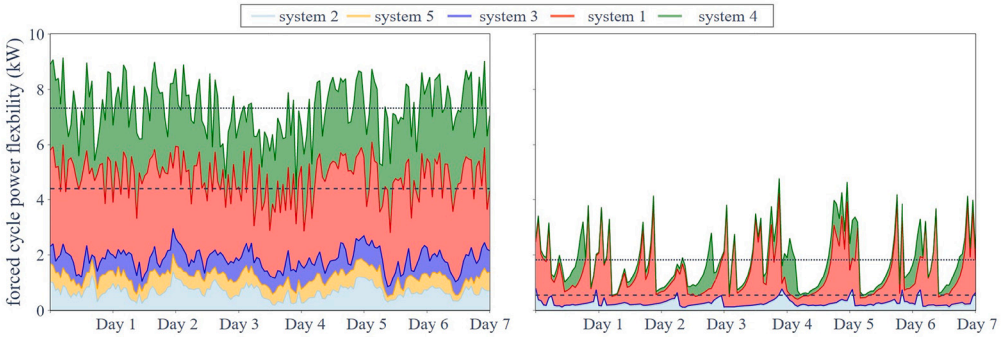


**Fig. 10.** Stacked area plot for forced cycle power flexibility of all 5 systems in winter (left) and summer season (right). The stacked systems show single and aggregated quantity of the available flexibility. Dashed lines indicate the minimum aggregated flexibility, while the dotted lines represent the average aggregated flexibility.

It shows that the systems provide flexibility with respect to HP power and user demand.

### 3.3. Flexibility aggregation

Aggregation of single HP flexibilities spawns the ability of the aggregator to trade with them. Even though the actual application is out of scope of this study, we aggregated the power and energy flexibilities of the five HP systems from a small Central European region (Vorarlberg, Austria). The HP systems are single operated, and thus, do not consider the adjustment to other HPs' load. Hence, the coincidence of HP systems is not investigated in detail.

Fig. 8 shows the box plots for the forced (left) and delayed cycle power flexibility (right). The comparison of forced and delayed power flexibility, expressed as ratio, shows that the forced power flexibility is between 11 and 94-fold higher in average than in the delayed case. Thereby, system 1 and 4 can provide the highest share of flexibility. The sum of all systems results in an average power flexibility for the forced case of 4.3 kW with a maximum at 9.6 kW. Opposing, the delayed case shows an average of 0.02 kW, peaking at 0.4 kW.

However, as the box plots represent a one year period, seasonal variations are hardly distinguishable. Since the forced cycle power case attains more potential than the delayed case, we investigated the seasonal variation of the forced case for a one week period in winter and summer, cf. Fig. 10. The stack area plot shows each system's potential, as well as the aggregated potential of all single systems as sum. In the winter week (left), systems 1 and 4 show a high power potential of around 3 kW compared to all other systems. The aggregation of all systems shows an average of 7.3 kW (dotted), while a minimum of 4.4 kW (dashed) is always attainable. In the summer week (right) the overall potential is more than 4-times less compared to the winter scenario. Hereby, the permanently available power of 4.4 kW in winter, represents roughly the maximum in summer. While, a power of 0.8 kW (dashed) is permanently available, the average lays around 1.8 kW (dotted) in summer. The flexibility pattern in summer indicates more peaks, which is the result of no SH use, and highly volatile DHW use. In winter SH use leads to a more steady flexibility pattern, and up to four times more forced potential.

To summarize, we estimated the temporal, power and energy flexibility of a HP pool. Furthermore, the impact on the flexibility by seasonal variation and increment of temperature boundaries in the TES was investigated. We aggregated the power flexibilities of each single system to obtain insight on the achievable potential of the HP pool. Results led to the following main observations:

- For the temporal flexibility of the single system, the delayed case shows a 4-fold higher potential than the forced case. Moreover, if temperature spreads in the TES are increased by 5 Kelvin, the temporal flexibility potential almost doubles.
- The investigation of the cycle power flexibility reveals a trend opposed to the results gained for the temporal flexibility. In terms of power flexibility, results show that the forced case exceeds the delayed potential by a factor of ten. Further, seasonal variations halve the average potential of both cases from winter to summer. This can be attributed to the higher demand in winter including SH use.
- Seasonal variations impact all cycle power flexibilities of the HP pool, as the forced and the delayed potential in each case more than halves in summer compared to winter season. This behaviour is referable to one mentioned above.
- The aggregation of the cycle power flexibilities leads to an yearly average in the forced case of about 4.3 kW and 0.02 kW in the delayed case, respectively. Investigating seasonality clarifies that the maximum achievable power in summer is achievable all the time in winter ($\approx$ 4.4 kW).
- Likewise to the power flexibility, the forced energy flexibility shows a bigger potential than the delayed case. Even though the cycle times are 5-fold in the delayed case, this does not result in the same amount of available energy flexibility than in the forced case. Derived from that, it seems obvious that the forced flexibility leads to a higher storage exploitation (210-2700 full charging cycles) than the delayed case (1-3 full depletion cycles).
- Available flexibility varies in each system, even though system specifications, e.g., compressor class, are similar. A high dependency on system setup and user behaviour shows the clear necessity of a device and user-specific estimation method for flexibility. A method based on data collected in the field, as the one proposed, provides such capabilities.

## 4. Conclusions

The utilization of HP flexibilities can help balancing the grid via DSM measures and lets flexibility providers benefit financially. However, participation for end customers in the flexibility market is only possible via an aggregator. The aggregator aims maximizing his trading profits via provision of coupled HP flexibilities. To determine, how much flexibility (power and energy) a set of HPs provides, the aggregator needs a transferable method with distinction of DHW and SH. Additionally, the method must be real-world applicable, thus able to incorporate reduced sensor and system information. To this day, literature covers a big number of specific flexibility estimation methods, but a unique definition does not exist.

Therefore, we extended a promising method from literature to distinguish between DHW/SH use and incorporate reduced sensor information. Furthermore, we applied the method to real-world data of five single HP systems to prove the transferability. We were able to identify the individual user demand, the heat transfer characteristics, and the

dimensioning of each system, as well as to quantify the flexibility of the HP pool and of each subsystem.

Results show the potential of the forced power- and energy flexibility of each system compared to the delayed cases being significantly higher. Likewise, seasonal changes have to be considered, as in summer no SH use decreases the available power- and energy flexibility. The integration of space cooling might solve this problem and reduce the flexibility decrease in summer.

As the available flexibility varies in each system dependent on the system setup and the user behaviour, the necessity of a system-specific flexibility estimation method is shown.

From the method and the results obtained, the aggregator is able to derive the information necessary to market the flexibilities.

## Declaration of competing interest

The authors declare that they have no known competing financial interests or personal relationships that could have appeared to influence the work reported in this paper.

## Data availability

Data will be made available on request.

## Acknowledgements

The financial support by the Austrian Federal Ministry for Digital and Economic Affairs and the National Foundation for Research, Technology and Development and the Christian Doppler Research Association is gratefully acknowledged. The authors are grateful to the project partner Weider Wärmepumpen GmbH for providing the real data.

## References

Arteconi, A., Polonara, F., 2018. Assessing the demand side management potential and the energy flexibility of heat pumps in buildings. Energies 11 (7), 1846. https://doi.org/10.3390/en11071846.

Arteconi, A., Hewitt, N., Polonara, F., 2013. Domestic demand-side management (DSM): role of heat pumps and thermal energy storage (TES) systems. Appl. Therm. Eng. 51 (1–2), 155–165. https://doi.org/10.1016/j.applthermaleng.2012.09.023.

Baumann, C., Huber, G., Alavanja, J., Preißinger, M., Kepplinger, P., 2023. Experimental validation of a state-of-the-art model predictive control approach for demand side management with a hot water heat pump. Energy Build. 285, 112923. https://doi.org/10.1016/j.enbuild.2023.112923.

Chen, Y., Xu, P., Gu, J., Schmidt, F., Li, W., 2018. Measures to improve energy demand flexibility in buildings for demand response (DR): a review. Energy Build. 177, 125–139. https://doi.org/10.1016/j.enbuild.2018.08.003.

Clauß, J., Finck, C., Vogler-Finck, P., Beagon, P., 2017. Control strategies for building energy systems to unlock demand side flexibility – a review. In: IBPSA Building Simulation 2017. San Francisco, pp. 1–10.

Devriese, J., Degrande, T., Mihaylov, M., Verbrugge, S., Colle, D., 2019. Techno-economic analysis of residential thermal flexibility for demand side management. In: 2019 CTTE-FITCE: Smart Cities & Information and Communication Technology (CTTE-FITCE). IEEE, Ghent, Belgium, pp. 1–6.

D'hulst, R., Labeeuw, W., Beusen, B., Claessens, S., Deconinck, G., Vanthournout, K., 2015. Demand response flexibility and flexibility potential of residential smart appliances: experiences from large pilot test in Belgium. Appl. Energy 155, 79–90. https://doi.org/10.1016/j.apenergy.2015.05.101.

EN 14511-3:2022, 2022. Air conditioners, liquid chilling packages and heat pumps for space heating and cooling and process chillers, with electrically driven compressors - Part 3: Test methods Standard, European Committee for Standardization.

Fischer, D., Wolf, T., Wapler, J., Hollinger, R., Madani, H., 2017. Model-based flexibility assessment of a residential heat pump pool. Energy 118, 853–864. https://doi.org/10.1016/j.energy.2016.10.111.

Gade, P.A.V., Skjøtskift, T., Bindner, H.W., Kazempour, J., 2022. Market model 3.0: a new ecosystem for demand-side flexibility aggregators in Denmark. arXiv:2209.02332 [cs, eess]. https://doi.org/10.48550/arXiv.2209.02332.

Hewitt, N.J., 2012. Heat pumps and energy storage – the challenges of implementation. Appl. Energy 89 (1), 37–44. https://doi.org/10.1016/j.apenergy.2010.12.028.

Iria, J., Soares, F., Matos, M., 2019. Optimal bidding strategy for an aggregator of prosumers in energy and secondary reserve markets. Appl. Energy 238, 1361–1372. https://doi.org/10.1016/j.apenergy.2019.01.191.

Jensen, S.O., Marszal-Pomianowska, A., Lollini, R., Pasut, W., Knotzer, A., Engelmann, P., Stafford, A., Reynders, G., 2017. IEA EBC annex 67 energy flexible buildings. Energy Build. 155, 25–34. https://doi.org/10.1016/j.enbuild.2017.08.044.

Kepplinger, P., Huber, G., Petrasch, J., 2015. Autonomous optimal control for demand side management with resistive domestic hot water heaters using linear optimization. Energy Build. 100, 50–55. https://doi.org/10.1016/j.enbuild.2014.12.016.

Kuboth, S., Heberle, F., Weith, T., Welzl, M., König-Haagen, A., Brüggemann, D., 2019. Experimental short-term investigation of model predictive heat pump control in residential buildings. Energy Build. 204, 109444. https://doi.org/10.1016/j.enbuild.2019.109444.

Kuboth, S., Weith, T., Heberle, F., Welzl, M., Brüggemann, D., 2020. Experimental long-term investigation of model predictive heat pump control in residential buildings with photovoltaic power generation. Energies 13 (22), 6016. https://doi.org/10.3390/en13226016.

Li, H., Wang, Z., Hong, T., Piette, M.A., 2021. Energy flexibility of residential buildings: a systematic review of characterization and quantification methods and applications. Adv. Appl. Energy 3, 100054. https://doi.org/10.1016/j.adapen.2021.100054.

Marijanovic, Z., Theile, P., Czock, B.H., 2022. Value of short-term heating system flexibility – a case study for residential heat pumps on the German intraday market. Energy 249, 123664. https://doi.org/10.1016/j.energy.2022.123664.

Nuytten, T., Claessens, B., Paredis, K., Van Bael, J., Six, D., 2013. Flexibility of a combined heat and power system with thermal energy storage for district heating. Appl. Energy 104, 583–591. https://doi.org/10.1016/j.apenergy.2012.11.029.

Olivella-Rosell, P., Lloret-Gallego, P., Munné-Collado, I., Villafafila-Robles, R., Sumper, A., Ottessen, S.O., Rajasekharan, J., Bremdal, B.A., 2018. Local flexibility market design for aggregators providing multiple flexibility services at distribution network level. Energies 11 (4), 822. https://doi.org/10.3390/en11040822.

Pean, T., Costa-Castello, R., Fuentes, E., Salom, J., 2019. Experimental testing of variable speed heat pump control strategies for enhancing energy flexibility in buildings. IEEE Access 7, 37071–37087. https://doi.org/10.1109/ACCESS.2019.2903084.

Stinner, S., 2018. Quantifying and aggregating the flexibility of building energy systems. Ph.D. thesis. RWTH Aachen University. ISBN: 9783942789554 OCLC: 1075122288.

You, Z., Zade, M., Kumaran Nalini, B., Tzscheutschler, P., 2021. Flexibility estimation of residential heat pumps under heat demand uncertainty. Energies 14 (18), 5709. https://doi.org/10.3390/en14185709. https://www.mdpi.com/1996-1073/14/18/5709.

Zeiselmair, A., Köppl, S., 2021. Constrained optimization as the allocation method in local flexibility markets. Energies 14 (13), 3932. https://doi.org/10.3390/en14133932. https://www.mdpi.com/1996-1073/14/13/3932.